AJP

ISSN : 0971 - 3093

Vol 32, Nos 9 - 12, September-December, 2023

ASIAN JOURNAL OF PHYSICS

An International Peer Reviewed Research Journal

Advisory Editors : W Kiefer, FTS Yu, Maria J Yzuel

Special issue in honour of Prof Baidyanath Basu

Prof Baidyanath Basu

Guest Editor : Subrata Kumar Datta

ap

ANITA PUBLICATIONS

FF-43, 1st Floor, Mangal Bazar, Laxmi Nagar, Delhi-110 092, India

B O : 2, Pasha Court, Williamsville, New York-14221-1776, USA

Asian Journal of Physics
Vol. 32, No 12 (2023) 453-462
Available on: www.asianjournalofphysics.com

ap

A simple and fast split-model optimization technique for RF couplers of helix traveling-wave tubes

Raktim Guha[1,2] and Sanjay Kumar Ghosh[1,2]

[1]*Academy of Scientific and Innovative Research* (*AcSIR*), *Ghaziabad- 201 002*, *India*
[2]*Vaccum Electron Devices Group, CSIR-CEERI*, *Pilani-333 031*, *India*

Dedicated to Prof B N Basu

A simple and fast split-model technique based on analysis and simulation was developed for the optimization of the RF coupling system of a helix traveling-wave tube (TWT). The proposed technique addresses the tedious design of RF power coupling to a non-uniform helix pitch section of the slow-wave structure of the TWT that becomes all the more tedious if one uses an H-plane end-launcher transition rather than an E-plane launcher, such as, probe or door-knob type of transition to reduce the size of the coupling system with better S-parameters. This proposed split-model optimization technique significantly reduced the optimization time by > 95% as compared to the conventional optimization technique without sacrificing the desired accuracy in the value of voltage standing wave ratio (VSWR). The proposed technique yielded the value of VSWR close to that predicted by the conventional optimization technique. © Anita Publications. All rights reserved.

Keywords: Coaxial couplers, Rectangular waveguide transition, Impedance matching, Helix slow-wave structure (SWS), Traveling wave tube (TWT).

doi.10.54955/AJP.32.9-12.2023.453-461

1 Introduction

Helix traveling-wave tubes (TWTs) find wide range of applications in communication, radar and electronic warfare. Along with the design of a TWT one needs to pay due attention in designing the RF power coupling systems of the device also. Consequently, efforts have been made in designing the RF coupling system to meet the challenging task of fulfilling the requirement of wide bandwidth and high power handling capability. However, while addressing these issues, one needs to include the effect of attenuator coated dielectric helix-support rods, uniform/ non-uniform helix pitch, and isotropic/ anisotropic metal envelope for proper transformation of helix characteristic impedance with the external load and RF plumbing impedance [1-7].

In the conventional analytical design approach, the characteristic impedance of a complex helical slow-wave structure (SWS) as obtained by equivalent circuit analysis [8] is matched with the external load through the couplers using several simplifying assumptions [1,3,8]. However, due to oversimplified conventional approach, the voltage-standing wave ratio (VSWR) predicted by such analytical approach largely deviates from the experimental results. This motivated the designers to lean towards commercially available 3-D electromagnetic simulation tools, such as CST [9] and HFSS [10]. However, the modelling of coupling system in commercial software packages also demands more computational time for each iteration irrespective of the system geometry, and this issue gets further aggravated if one reduces the mesh size for

Corresponding author
e mail: raktim.guha01@gmail.com (Raktim Guha)

better accuracy [1,7]. To overcome these limitations, a split-model (SM) optimization technique of couplers has been proposed in [5] to reduce the optimization time. In split-model (SM) optimization technique [5], one needs to design and simulate a number of helix models and the same number of coupler assemblies for reflection coefficients with different port and load impedances, respectively, typically, 50, 55, 60, ... Ω, etc., Subsequently, the simulated results of S-parameters are combined analytically. Thus, this approach needs several iterative trials to obtain the desired value of VSWR and consequently this technique also takes relatively longer time to optimize the coaxial couplers. These limitations of the SM technique [5] have been alleviated in the proposed improved SM technique presented in this paper by eliminating several numbers of simulation pairs of the old SM technique. The improved approach reduces the optimization time by about 90%. Here, the optimization process has been implemented in a two-section helix SWS having uniform and non-uniform helix pitches at input and output sections, respectively. The input coupler is terminated in sub-miniature A (SMA) type connector, while the output coupling system is an H-plane end-launcher transition of a rectangular waveguide through an SMA connector (Fig 1).

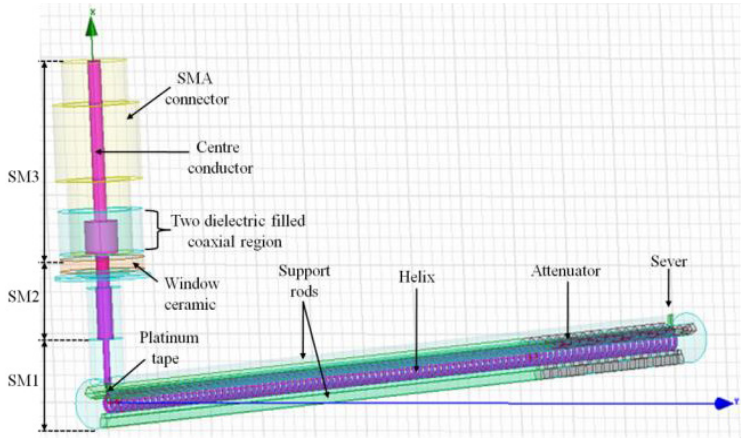

(a)

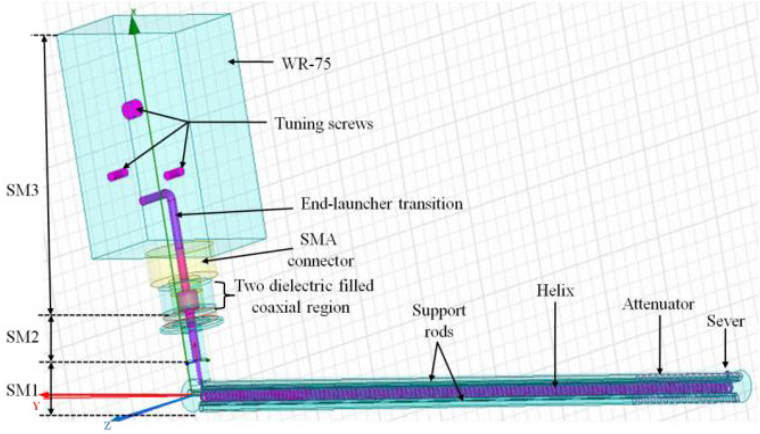

(b)

Fig 1. The model of helix TWT along with (a) input section with SMA connector and (b) output section with H-plane end-launcher transition followed by SMA connector.

In order to achieve the desired accuracy in results, the attenuator coating loss on dielectric helix-supports has been modelled by an equivalent bulk-conductivity, using the piece-wise model [6,11] and also the coupler-to-helix transition discontinuity has been considered [6] in the proposed SM technique. In section 2, the proposed SM technique has been described. Results are presented and discussed in section 3 and conclusions are given in section 4.

2 Proposed split-model optimization technique

In the conventional optimization modelling technique, the SWS, coupler, window, connector/ waveguide, etc. are considered as a single integral model which requires a large number of mesh cells for accurate results and takes very long iteration time [1-3]. However, by removing the SWS from the integrated model and splitting it into different matched sections, one can reduce the iteration/ simulation time significantly with desired accuracy. Thus, in this proposed model, the SWS and the transition section have been replaced with their respective input impedances. Thus, the proposed optimization technique as applied to the model of the helix with the coupling system (Fig 1) comprises three split-models for both input and output coupling systems as: (i) split-model 1 (SM1) consisting of the helix SWS supported by attenuator-coated dielectric rods, sever, and coaxial transition section; (ii) split-model 2 (SM2) consisting of the coaxial coupler with the ceramic window assembly; and (iii) split-model 3 (SM3) consisting of SMA connector at the input section and the SMA to H-plane end-launcher type coupling transition of the rectangular waveguide at the output section.

The length and radius of the helix-to-coupler transition section are optimized in HFSS and verified in CST to get the best possible VSWR at port 1 of SM1 over the band. For this, one needs both the real and imaginary parts of the input impedance ($Z_{in\_SM}(f)$) at port 1 (Fig 2(a) and 2(c)) for both input and output sections and are stored in excel sheets to recall during the process of optimization. This approach enables one to replace SM1, reducing the total number of mesh cells (Table 1) during optimization of SM2 and SM3.The stored impedance ($Z_{in\_SM1}(f)$) of SM1 in excel sheet is used as the load impedance at port 2 of SM2 ($Z_{l\_SM3}(f)$) which helps one to optimize the dimensions of SM2 quickly for better VSWR. Similarly, the modelling of SM3 can easily be optimized taking ($Z_{in\_SM2}(f)$) at port 3 (Figs 2(b) and 2(d)) and at port 4, as load impedances, respectively, to get the desired VSWR. After completing the design of SM2 and SM3 analytically, one can model SM2 and SM3 integrated with SM1 in HFSS and CST to verify the optimized VSWRs, obtained analytically. Further, SM3 has been re-tuned for suitable VSWR at the output section by introducing the tuning screws (not considered in analysis) in the rectangular waveguide. The proposed optimization method is simpler and faster than the conventional optimization methods [1-6] as well as the SM optimization method in [5].

A. Analytical approach

$$Z_{in\_SM1\_ip/op}(f) = R_{in\_SM1\_ip/op}(f) + JX_{in\_SM1\_ip/op}(f) \tag{1}$$

where $Z_{in\_SM1\_ip/op}(f)$ and $X_{in\_SM1\_ip/op}(f)$ are the real and imaginary parts of $Z_{in\_SM1\_ip/op}(f)$, respectively, and the subscripts *ip* and *op* refer to the input and output sections, respectively. The impedance obtained from Eq (1) acts as the load impedance of SM2. Thus, the load impedance of SM2 at port 2 is:

$$Z_{l2\_SM2}(f) = Z_{in\_SM1}(f) \tag{2}$$

The characteristics impedance at each section of the coaxial line of SM2 (Fig 1) can be defined as [12]:

$$Z_{0t\_SM2} = 60/(\varepsilon_{rt\_SM2})^{1/2}\ ln\ (d_{t\_SM2}/r_{t\_SM2} \tag{3}$$

where t = 1, 2, 3, ... refer to the sections of SM2. Z_{0t_SM2}, ε_{rt_SM2}, d_{t_SM2} , and r_{t_SM2} are the characteristic impedance, relative permittivity, radii of the outer and inner conductors of the coaxial line of the t^{th} section of SM2, respectively. Thus, one can define input impedance of the p^{th} port using (Eq 3) as:

$$Z_{inp\_SM2}(f) = Z_{0t\_SM2}\,(Z_{l2\_SM2} + jZ_{0t\_SM2}\tan\beta l_{t\_SM2})/\,(Z_{0t\_SM2} + jZ_{l2\_SM2}\tan\beta l_{t\_SM2}) \tag{4}$$

Here, $p = 3, 5, 7, \ldots$ and $\beta\ (= 2\pi f/c)$ is the propagation constant in free space with f being the operating frequency and c being the velocity of light in free space; l_{t_SM2} is the length of the coaxial line of the t^{th} section. Now, $Z_{inp\_SM2}(f)$, obtained from (Eq 4), will act as the load impedance at $(p + 1)^{th}$ port of SM2, hence (Eq 2) can be rewritten as:

$$Z_{l(p+1)\_SM2}(f) = Z_{inp\_SM2}(f) \tag{5}$$

Similarly, the input impedance of respective sections can be calculated using Eq (4) by replacing $Z_{l2\_SM2}(f)$ with $Z_{l(p+1)\_SM2}(f)$, and, finally, VSWR of the p^{th} port can be obtained as:

$$\text{VSWR} = (1 + |\Gamma_{p\_SM2}|)/(1 - |\Gamma_{p\_SM2}|) \tag{6}$$

here, $\Gamma_{p\_SM2} = (Z_{lp\_SM2} - Z_{0t\_SM2})/\,(Z_{lp\_SM2} + Z_{0t\_SM2})$ is the reflection coefficient of the t^{th} section of SM2.

However, for SM3, of both the input and the output sections, one needs to consider the presence of two additional dielectrics (boron nitride and air) due to the SMA connector over the top of the window assembly in the model (Fig 1). The characteristic impedance of SM3, treated as a two-dielectric-filled coaxial line, can be then put as [13]:

$$Z_{0t(n=2)\_SM3} = \frac{1}{2\pi\varepsilon_0 c}\left[\ln\left(\frac{R_{t(n=2)\_SM3}}{r_{t\_SM3}}\right) \times \left\{\frac{\varepsilon_{rt(n=2)\_SM3}\ln\left(R_{t(n=1)\_SM3}/r_{t\_SM3}\right) + \varepsilon_{rt(n=1)\_SM3}\ln\left(R_{t(n=2)\_SM3}/R_{t(n=1)\_SM3}\right)}{\varepsilon_{rt(n=1)\_SM3}\,\varepsilon_{rt(n=2)\_SM3}}\right\}\right]^{1/2} \tag{7}$$

here, $R_{t(n=2)\_SM3}$ and $R_{t(n=1)\_SM3}$ are the radii of the outer and inner dielectrics of t^{th} section, respectively; $\varepsilon_{rt(n=2)\_SM3}$ and $\varepsilon_{rt(n=1)\_SM3}$ are the relative permittivity of the outer and inner dielectrics of the t^{th} section, respectively; and r_{t_SM3} is the radius of the central conductor of SM3.

Furthermore, in the output section of the model, a rectangular waveguide with H-plane end-launcher type coupling loop is fixed over the SMA connector (Fig 1(b)). This end-launcher type coupling loop excites TE modes (while current following along the vertical arm) and TM modes (while current following along the horizontal arm). Therefore, hybrid modes exist in the end-launcher type coupler [14]. By considering the higher order modes, one can express the input impedance seen by the SMA connector driving the end-launcher as:

$$Z_{in\_wg\_SM3}(f) = \frac{1}{4\pi^2 ab\cos^2(\beta(L_1 + L_2))}\left[\sum_{m=1}^{\infty}\sum_{n=0}^{\infty}\left\{\frac{d_n\beta^2}{\beta_{wg}}A_{mn}^2\sin(m\pi x_0/a)(B_{mn,1} + B_{mn,2})C_{mn}D_{mn}\right\} - \sum_{m=1}^{\infty}\sum_{n=1}^{\infty}\left\{\frac{E_{mn}^2}{\beta_{wg}(\beta^2 + \beta_{wg}^2)}(F_{mn,1} + F_{mn,2} + F_{mn,3})\right\}\right] \tag{8}$$

here, β and β_{wg} are the propagation constants of the free-space region and the rectangular waveguide, respectively; a and b are the broad-wall and narrow-wall dimensions of the rectangular waveguide, respectively; L_1 and L_2 are the lengths of the end-launcher parallel and perpendicular to the broad wall, respectively; and x_0 is the distance of the end-launcher from the narrow wall of the waveguide. The parameters d_n, A_{mn}, $B_{mn,1}$, $B_{mn,2}$, C_{mn}, D_{mn}, E_{mn}, $F_{mn,1}$, $F_{mn,2}$, and $F_{mn,3}$, are to be interpreted as in [14]. The VSWR of the waveguide can be calculated using Eq (8) as:

$$\text{VSWR} = (1 + |\Gamma_{wg\_SM3}|)/(1 - |\Gamma_{wg\_SM3}|) \tag{9}$$

with

$$T_{wg} = (Z_{in\_wg\_SM3}(f) - Z_{inp\_SM3}(f))/(Z_{in\_wg\_SM3}(f) + Z_{inp\_SM3}(f))$$

B Simulation Approach

For this, one needs to discretize the operating frequency band into some frequency points. The input impedance of the respective frequency points can be obtained from the excel sheet (as mentioned above). Thus, one can directly apply the values of the input impedances of SM1 (or SM2) as the load impedance of SM2 (or SM3) using the post processing option in HFSS. After a number of iterations, one can achieve the desired VSWR responses of SM2 and SM3 (Figs 3(b-c) and Figs 4(b-c)) (see section 3).

3 Results and Discussion

The effectiveness of the proposed simplified SM optimization method has been investigated for both the input coupler with SMA connector and the output coupler with SMA connector and connector to H-plane rectangular waveguide transition as used in an X-band TWT. The values of VSWR, obtained by this proposed approach of both the input and output couplers have been compared with those obtained by the conventional optimization method. First, the input and output coupling structures (SM2) have been modelled analytically considering input impedance, of SM1 of both input and output section (Fig 2(a)-(c)), respectively, as load impedance of SM2 as per the proposed method and then they are simulated using the conventional method. A very good agreement within 6-10% between them was observed. In a similar way, SM3 of both input and output sections have been modelled considering input impedance of SM2 of both input and output sections (Fig 2(b-d)), respectively, as load impedance of SM3.

Table 1. Comparison of conventional method and the proposed simplified split-model optimization method

Parameters	Time taken by each simulation		Total number of mesh cells	
	CST	HFSS	CST	HFSS
SM1	~ 3 hr 50min	~ 1 hr 05 min	13313300	215867
Conventional method (SM1 + SM2)	~ 5 hr 10min	~ 1 hr. 20 min	17578034	289336
Proposed method (SM2 only)	—	~ 1min	—	22540
Conventional method (SM1 + SM2 + SM3)	~ 6 hr 40min	~ 1 hr 45 min.	25286250	325019
Proposed method (SM3 only)	—	~ 1min50 sec	—	41042

Moreover, the proposed method reduces the optimization time by more than 95% as compared to the time required by the conventional method. The obtained values of VSWR and the optimization time are shown in Figs 3 and 4 and Table 1, respectively.

The real and imaginary parts of the input impedances of SM1 for both input and output sections (Fig 2(a) and 2(c)), and SM2 of both the input and output sections have been modelled and optimized analytically using Eqs (1-6). The optimized values of VSWR of SM2 agree closely with those obtained

from using the conventional approach (Fig 3(b) and 4(b)). Thus, with reference to the input section, one can obtain the optimized values of VSWR of SM3 (Fig 3(b) and 4(b)) using Eqs (1-7) together with the data of the input impedance obtainable from Fig 2(b). Similarly, with reference to the output section, one can use Eqs (1-9) and the data of the input impedance obtainable from Fig 2(d) to find VSWR (Figs 3(c) and 4(c)). Not very close agreement between the analytical and simulated results (Fig 3(c) and 4(c)) can be attributed to the non-excitation of pure TEM mode in the two-dielectric coaxial line configuration of the model in both the input and output (Fig 1). Furthermore, the disagreement, more so at lower frequencies, also owes to the assumption of the excitation of only the dominant mode in the H-plane end-launcher transition in the output section. The impedance matching can be improved by inserting multiple tuning screws [15,16] as shown in (Fig 1(b)). Further, by adjusting the radius and height of the tuning screws inside the rectangular waveguide, one can achieve nearly flat VSWR response within the desired frequency band (Fig 4(d)). Also, the computational time required for the proposed method is very less and can be estimated easily in a normal desktop computer. Thus, through this study on the input and output coupling system of a helix TWT, it is established that the proposed simplified split-model optimization method yields better and flat VSWR of the system over the band of interest and at the same time it takes very less computational time.

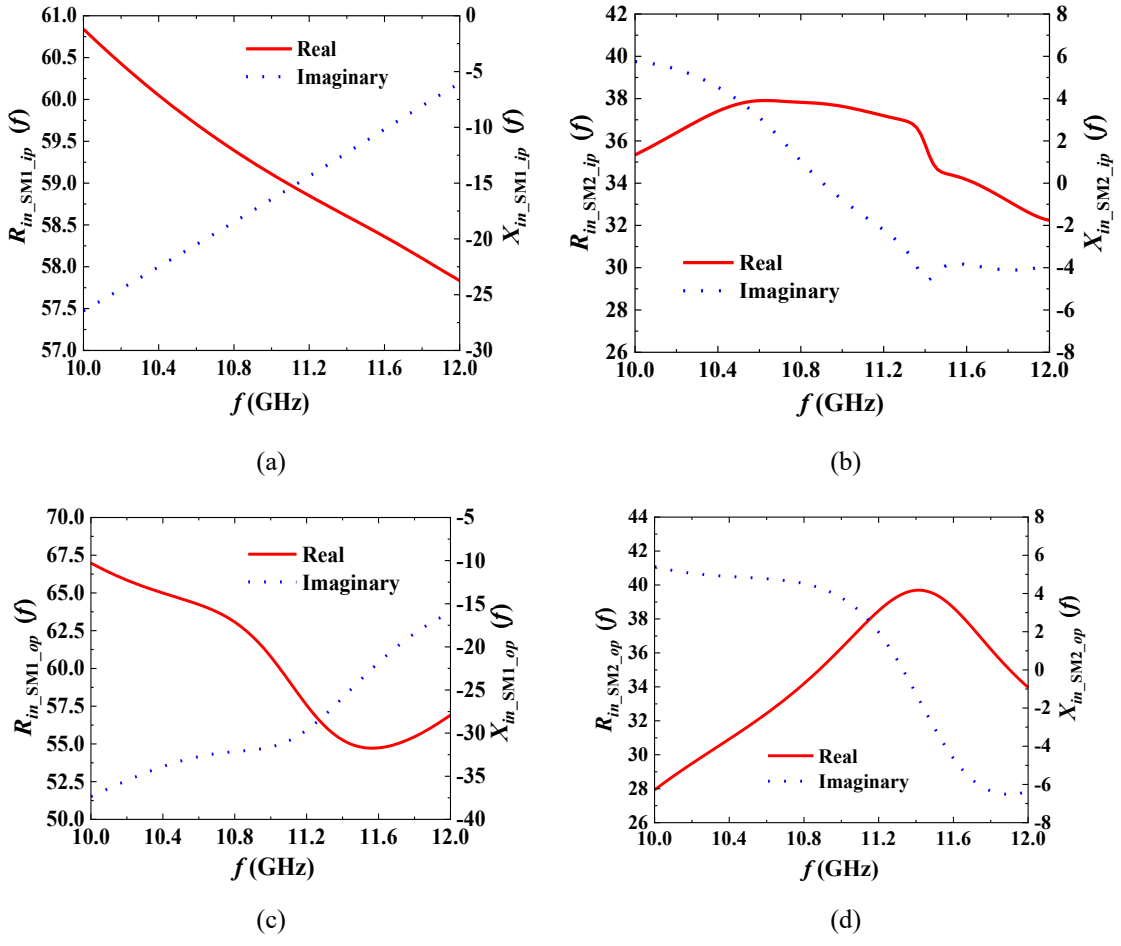

Fig 2. Real and imaginary parts of input impedance versus frequency of SM1 and SM2 for both the input (a-b) and output (c-d) couplers (Fig 1) integrated with SM1 as obtained using HFSS.

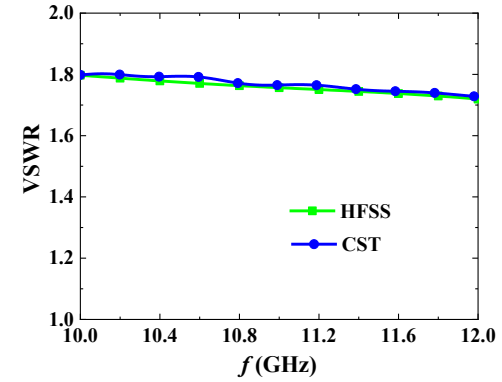

(a)

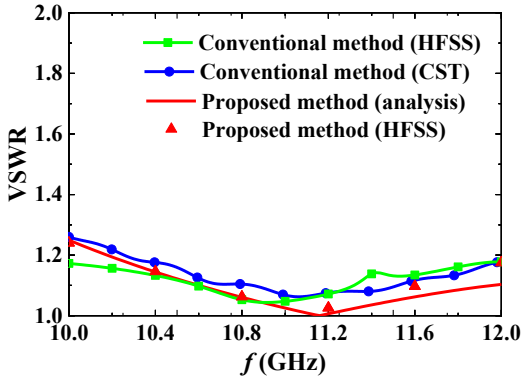

(b)

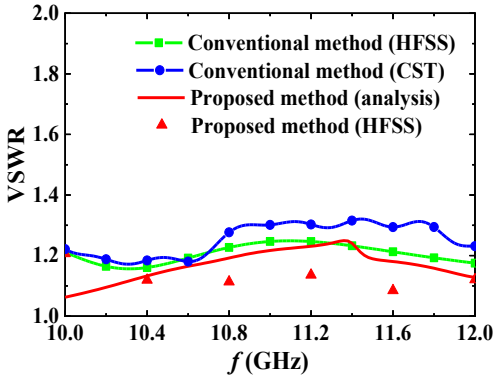

(c)

Fig 3. Comparison of VSWR versus frequency responses with reference to the input coupler: (a) SM1as obtained using HFSS and CST; (b) SM2 (inner conductor diameter of step 1 to 3 are 1.2 mm, 1.6 mm and 1 mm, respectively; total length is 14 mm; outer conductor diameter is 2.2 mm; window diameter 6.3 mm) and (c) SM3 (inner conductor diameter of step 1 and 2 are 2.4 mm and 1.2 mm, respectively; total length 10 mm; dielectric jacket diameter of steps 1 to 3 are 4 mm, 5.3 mm and 4 mm, respectively). The results correspond to SM2 and SM3 as obtained using the conventional method, using HFSS and CST, and the proposed optimization methods obtained by both analysis and HFSS.

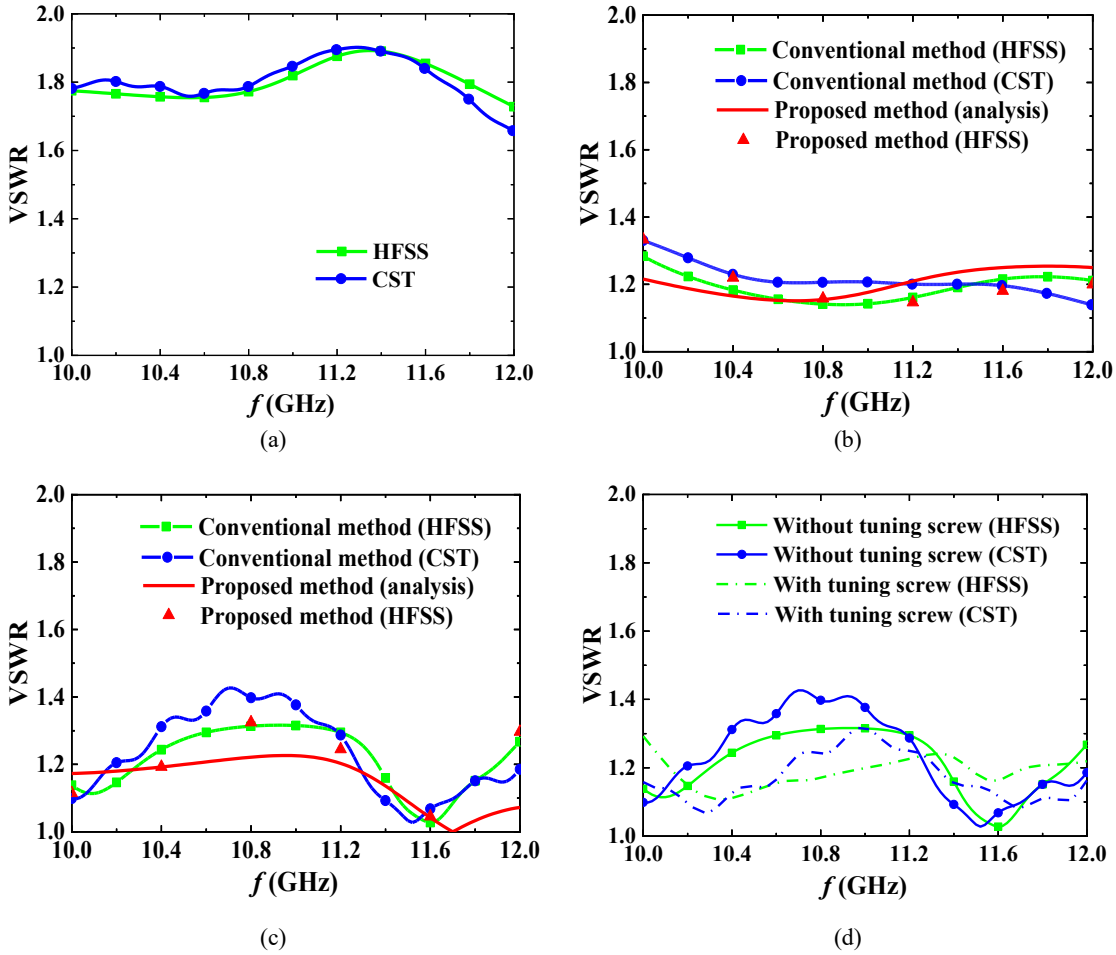

Fig 4. Comparison of VSWR versus frequency responses with reference to the input coupler: (a) SM1 as obtained using HFSS and CST; (b) SM2 (same as input SM2) and (c) SM3 (rectangular waveguide WR75, connector dielectric diameter of step 1 and 2 are 7.9 mm and 4 mm, respectively; total length is 6.5 mm; end-launcher horizontal arm and vertical arm lengths are 12.75 mm and 6.55 mm, respectively). SM2 and SM3 as obtained using conventional and proposed optimization method of output coupler and H-plane coupled coaxial to rectangular waveguide transition (without any tuning screw); (d) considering tuning screws for further impedance matching.

4 Conclusion

A simplified split-model optimization method has been proposed for the optimization and design of the coupling system of a helix TWT. The proposed method is faster than the other methods in vogue in yielding results. However, there is scope to improve the analysis by taking into account losses in the transmission line model in the analysis. The future scope also includes the validation of the VSWR of the coupling system predicted by the proposed optimization method against experimental measurement.

Acknowledgement

The authors are thankful to the Director, CSIR-CEERI, Pilani, Rajasthan, India for allowing us to publish this work.

References

1. Jia B, Baik C.-W, Park G.-S, The design of the input and output transformer for wideband helix TWT, in Proc 2nd International Conference on Microwave and Millimeter Wave Technology, Beijing, China, September 2000,, (2000)715–719, doi: 10.1109/ICMMT.2000.895787.
2. Sinha A K, Singh V V P, Srivastava V, Joshi S N, On the design of coaxial coupler having multi-section short transformer for compact sized power helix traveling wave tubes, in Proc Int Vac Electron Conf, (2000),p2.25–p 2.26; doi: 10.1109/OVE:EC.2000.847499.
3. Agarwal A K, Raina S, Kumar L, A novel approach for simulation of coaxial coupler for helix TWTs using HFSS, in Proc 4th IEEE Int Vacuum Electron Conf, (2001)58–59; doi: 10.1109/IVEC.2011.5746942.
4. Duffield M J, A technique for designing the RF connectors used on Helix TWTs, in Proc IEEE Int Vac Electron Conf (IVEC), (2007)1–2; doi: 10.1109/IVELEC.2007.4283389.
5. Ghosh T K, Carter R G, Challis A J, Rushbrook K G, Bowler D, Optimization of Coaxial Couplers, *IEEE Trans Electron Devices*, 54(2007)1753–1769.
6. Rao K V, Naidu V B, Rao P R R, Datta S K, Simulation of RF coupler of a multi-section TWT with matched sever-loss," 2009 IEEE International Vacuum Electronics Conference, (2009)455-456, doi: 10.1109/IVELEC.2009.5193567.
7. Rao P R R, Datta S K, Kumar L, Optimization of Couplers of TWT using TDR Method, in Proc IEEE Int Vac Electron Conf (IVEC), (2012)79–80; doi: 10.1109/IVEC.2012.6262082.
8. Jain P K, Basu B N, Electromagnetic wave propagation through helical structures, in Electromagnetic Fields in Unconventional Materials, (Eds) Singh O N, Lakhtakia A, (Hoboken, NJ, USA: Wiley), 2000.
9. CST AG, Darmstadt, Germany. CST STUDIO SUITE. Accessed: 2018. [Online]. Available: www.cst.com.
10. HFSS V18.0: Ansoft Corporation. www.ansoft.com.
11. Naidu V B, Datta S K, Rao P R R, Agrawal A K, Reddy S U, Kumar L, Basu B N, Three-Dimensional Electromagnetic Analysis of Attenuator-Coated Helix Support Rods of a Traveling-Wave Tube, *IEEE Trans Electron Devices*, 56(2009)945–950.
12. Rizzi P A, Microwave Engineering: Passive Circuits. New Delhi: Prentice Hall International, 1988.
13. Li Q, Y. Zhang, L. Qu, Y. Fan, Quasi-Static Analysis of Multilayer Dielectrics Filled Coaxial Line Using Conformal Mapping Method, in Proc IEEE International Conference on Computational Electromagnetics (ICCEM), (2018)1–3, doi: 10.1109/COMPEM.2018.8496545.
14. Yang D.-Y, Design and Fabrication of an End-Launched Rectangular Waveguide Adapter Fed by a Coaxial Loop, *J Inf Commun Converg Eng*, 10(2012)103–107.
15. Gesche R, Löchel N, Two Cylindrical Obstacles in a Rectangular Waveguide- Resonances and Filter Applications, *IEEE Trans Microw Theory Tech*, 37(1989)962–968.
16. Pandharipande V M, Das B N, Equivalent network of a variable-height post in a rectangular waveguide, *Proc Inst Electr Eng*, 124(1977)1160–1162.

[*Received*: 25.04.2023; *revised recd*: 16.11.2023; *accepted*: 26.12.2023]

Raktim Guha, received his B Tech and M Tech degrees, both from West Bengal Technical University in 2012 and 2015, respectively and pursuing his Ph D (AcSIR) at CSIR-Central Electronics Engineering Research Institute (CEERI), Pilani, Rajasthan, He worked as Senior Project assistant from 2017 to 2021 at CSIR-CEERI. His research interests are in the area of space-TWTs, and metamaterial-assisted vacuum electron devices.

Sanjay Kumar Ghosh, working as Chief Scientist and a Professor at CSIR-Central Electronics Engineering Research Institute (CEERI), Pilani Rajasthan, completed his M Sc Physics and Ph D in Microwave Engineering in 1991 and 1996, respectively, both from Banaras Hindu University (BHU). Before joining CSIR-CEERI in 2010, he was associated with Bharat Electronics Ltd (BEL), Bangalore over a decade. Being former executive of BEL, Bangalore, he was associated with the development and production of different types of microwave tubes of strategic importance. At CSIR-CEERI, he is associated with the development of different types of microwave tubes including helix traveling-wave tubes (TWTs) for on-board satellite application. He has published more than hundred research papers in peer reviewed journals and national/ international conference proceedings. His current research area is broadbanding of helix TWTs for satellite and strategic applications and also coordination of different courses in AcSIR.